JOURNAL OF GEOPHYSICAL RESEARCH, VOL. 112, D01302, doi:10.1029/2006JD007234, 2007

Effects of source temporal resolution on transport simulations of boreal fire emissions

Edward J. Hyer,[1,2] Eric S. Kasischke,[1] and Dale J. Allen[3]

Received 27 February 2006; revised 1 June 2006; accepted 30 August 2006; published 4 January 2007.

[1] The quality of temporal information from daily burned area inputs was evaluated using a transport and chemistry experiment. Carbon monoxide emissions from boreal forest fires were estimated using burned area inputs with daily resolution. Averaging of emissions data to create 30-day aggregate data reduced the variance by 80%, indicating a substantial loss of information. Data from Russia, Canada, and Alaska were tested for periodicity to uncover systematic gaps in daily data. Some evidence of periodicity was found in data from Alaska, where temporal information came from fire mapping by the Alaskan Fire Service. Autocorrelation decayed rapidly and nearly monotonically for Canada and Russia, where temporal information came from Advanced Very High Resolution Radiometer (AVHRR) satellite observations. Daily data as well as 7-day and 30-day aggregates were used as input to the University of Maryland Atmospheric Chemistry and Transport Model, and output was compared with CO observations from the Cooperative Air Sampling Network (CASN); continuous measurements from Mace Head, Ireland; and total column CO retrievals from the Measurement of Pollution in the Troposphere (MOPITT) instrument. CASN flask measurements showed no sensitivity to high-frequency variability in the source, indicating the effectiveness of the filtering protocol at ensuring only well-mixed air masses are sampled in this data set. Differences between daily and 7-day simulations were too small for quantitative comparison in any of the data. For cases where the differences were substantial, simulations using daily and 7-day average sources agreed better with observations than 30-day average sources.

Citation: Hyer, E. J., E. S. Kasischke, and D. J. Allen (2007), Effects of source temporal resolution on transport simulations of boreal fire emissions, *J. Geophys. Res.*, *112*, D01302, doi:10.1029/2006JD007234.

1. Introduction

[2] Boreal forest fires are a large and concentrated source of trace gases to the atmosphere. During large fire years, boreal fires can account for as much as 20% of global carbon monoxide (CO) production from biomass burning [*Kasischke et al.*, 2005], and have impacts even greater at high latitudes during the summer months [*Novelli et al.*, 2003; *Yurganov et al.*, 2004]. Fire activity is concentrated spatially: even in the largest fire years, less than 2% of the forested area in the boreal zone is affected. During any given year, the great majority of emissions come from a small fraction of the largest fires [*Stocks et al.*, 2002]. The temporal distribution of boreal fires is likewise uneven: the fire season extends from late April into September, but the majority of the area burned in most large fire events results from just a few days of intense activity [*Flannigan and Harrington*, 1988]. This spatial and temporal concentration of the source means that modeled atmospheric effects of these emissions will be strongly dependent on the resolution of the input data.

[3] Most global data sets for trace gas emissions provide monthly averages. In many cases, such as fossil fuel consumption, this is unavoidable due to data limitations. For biomass burning, however, the satellite data products used to monitor fire activity have sufficient coverage to supply daily data [*Kaufman et al.*, 1998; *Reid et al.*, 2004]. Application of daily data sources may have potential to improve model representation of biomass burning emissions for studies of transport and chemistry, especially for highly active wildfires in the boreal region [*Damoah et al.*, 2006; *Fromm et al.*, 2005].

[4] The use of daily data for monitoring of biomass burning has been a focus of remote sensing research for many years [e.g., *Malingreau and Grégoire*, 1996]. *Li et al.* [1997] evaluated daily Advanced Very High Resolution Radiometer (AVHRR) satellite observations of hot spot activity for monitoring boreal forest fires, and found that daily AVHRR data were in good agreement with ground-based observations of area burned in low cloud cover conditions. Satellite observations of active fires have known shortcomings for quantitative detection of burned area, including susceptibility to cloud cover, variable detection

[1]Department of Geography, University of Maryland, College Park, Maryland, USA.
[2]Now at Marine Meteorology Division, Naval Research Laboratory, Monterey, California, USA.
[3]Department of Atmospheric and Oceanic Science, University of Maryland, College Park, Maryland, USA.

0148-0227/07/2006JD007234$09.00

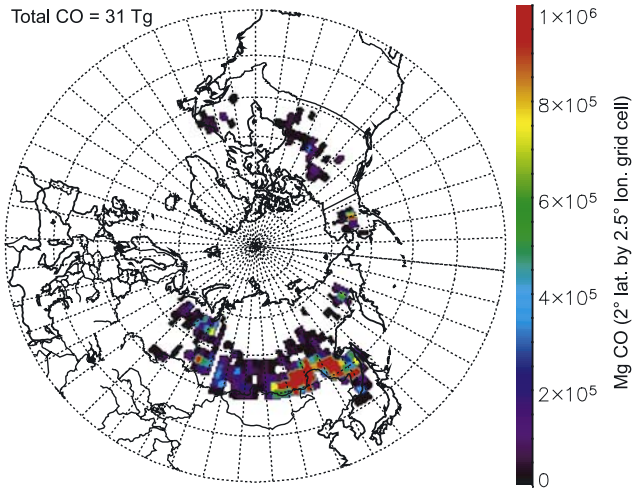

Figure 1. Carbon monoxide emissions from boreal forest fires in June–August 2000, in grams of CO, aggregated to a 2.5° longitude by 2° latitude grid.

efficiency, and numerous sources of false positives [see, e.g., *Kasischke et al.*, 2003; *Prins and Menzel*, 1994], but provide a valuable complement to other burned area information sources [*Fraser et al.*, 2000]. The high temporal resolution of active fire detection products allows better specification of the timing of fires than other methods [*Eva and Lambin*, 1998].

[5] *Heald et al.* [2003] used daily data from the World Fire Web (WFW) ([*Stroppiana et al.*, 2000]; for additional technical details see *Heald et al.* [2003]) to estimate daily fluctuations in biomass burning in southeast Asia. Heald et al. found that the WFW product, derived from AVHRR observations, had a strong dependence on scan angle, resulting in an effective sampling period of about eight days over tropical and subtropical Asia. To compensate for this incomplete sampling, Heald et al. used a persistence function to generate a continuous data set. Daily fluctuations derived in this manner were applied to monthly emissions estimates from *Duncan et al.* [2003] to generate a daily estimate of trace gas emissions, which was used as input to the GEOS-CHEM atmospheric transport and chemistry model. Comparison of GEOS-CHEM model results to observations from the TRACE-P experiment showed very small differences resulting from incorporation of daily data, with negligible impact on agreement between model and observations.

[6] There are a number of reasons why a similar analysis of boreal fires might not produce the same results. Fires in boreal forests have greater spatial and temporal variability than tropical fires, and the relative importance of brief periods of intense fire activity ("blow-ups") should enhance the atmospheric signal of day-to-day variability in emissions. From an observational perspective, the physical parameters of fire detection from space are quite different in the boreal zone [*Kasischke et al.*, 2003], and the coverage obtained from polar-orbiting satellites such as AVHRR is greater at high latitudes. The results of this study should clarify what temporal resolution of emissions data is necessary for accurate simulation of atmospheric transport of emissions from boreal forest fires.

[7] In this paper, daily boreal forest fire CO emissions from the Boreal Wildfire Emissions Model (BWEM-1) [*Kasischke et al.*, 2005] are used as input to model simulations of atmospheric CO evolution and transport. The effect of temporal aggregation on the gridded daily emissions product is examined to quantify high-frequency information in the daily data. A global chemistry and transport model (CTM) is used to simulate surface measurements of CO as well as CO retrievals from the Measurement of Pollution in the Troposphere (MOPITT) instrument, to determine whether daily data contributes significantly to agreement between models and measurements.

[8] To obtain a quantitative improvement in agreement between models and observations with daily inputs, three conditions must be satisfied: (1) The daily data must contain additional information not included in aggregate data; (2) this additional information must be accurate; and (3) the atmospheric simulation must be sensitive to high-frequency variability in the emissions source. This study evaluates directly the first and third conditions, and based on those results makes inferences about the accuracy of the high-resolution temporal information from the emissions model.

2. Data and Methods

2.1. Study Period and Region

[9] Boreal forest fire emissions during the 2000 fire season were the focus of this study. Area burned in the 2000 fire season (10.3×10^6 ha) was slightly lower than the annual average for 1996–2003 in the boreal forest (11.4×10^6 ha, based on data from [*Kasischke et al.*, 2005]). About 60% of boreal fire activity during 2000 occurred before 1 June, but early season comparisons were not made in this study because of interference from other Asian biomass burning sources geographically close to the boreal source. CO emissions from early season fires are included in the CTM simulations in this study and have some effect on measurements during the study period, but this influence is generally small and well mixed. Area burned during June–August 2000 was about 70% of the June–August average from 1996–2003. This study used atmospheric observations only from the high Northern Hemisphere (HNH, above 30°N).

2.2. CO Emissions Estimated by BWEM-1

[10] The BWEM-1 emissions model uses a flexible resolution GIS framework to integrate information on fire activity and fuels at a range of scales and produce emissions estimates at a range of resolutions [*Kasischke et al.*, 2005]. The BWEM-1 algorithm incorporates different fuel consumption parameters for early season, midseason, and late season fires. To avoid any artifacts in the temporal signal associated with transitions between these parameters, only the "midseason" parameters were used in this study. This resulted in higher emissions for fires in June and lower emissions for fires in August, compared with the "moderate" scenario reported by [*Kasischke et al.*, 2005]. Boreal fire CO emissions calculated in this fashion were 31 Tg for June–August 2000, 22% higher than the "moderate" scenario of *Kasischke et al.* [2005]. Figure 1 shows the

spatial distribution of CO emissions from boreal fires during June–August 2000.

2.3. Temporal Information in BWEM-1

[11] For this study, a daily estimate of CO emissions was prepared. This estimate was aggregated to produce 7-day and 30-day average emissions estimates. Information on timing of fires came from different sources depending on the region. Data sources for each region are described in this section.

2.3.1. Russia

[12] Area burned maps were generated at the Sukachev Institute of Forestry using AVHRR active fire detection as well as postfire burn scar mapping [*Sukhinin et al.*, 2004]. The active fire data were subsequently analyzed to produce separate temporal profiles of fire activity for each contiguous fire-affected area.

2.3.2. Canada

[13] The BWEM-1 was built to incorporate fire size and location data from the Canadian Large Fire Database [*Stocks et al.*, 2002], however this database only includes fires through 1999. For 2000 and later years, area burned in Canada was taken from data reported at the provincial level and collected by the Canadian Forest Service (available online at http://www.nrcan-rncan.gc.ca/cfs-scf/science/prodserv/firereport). Comparison between these data sources for 1995–1999 shows good agreement. Total area burned for each province is spatially distributed using the total annual density of hot spot detections from FireM3. FireM3 data for 2000 were derived from AVHRR data collected during daytime overpasses by NOAA-14, using a "best pixel" approach to reduce cloud contamination and avoid large scan angles [*Li et al.*, 1997]. The hot spot detections are clumped spatially into contiguous "fire-affected areas", and temporal profiles are calculated for each area. No operational data gaps appear in the 2000 data set, although hot spot detections from AVHRR are limited by cloud cover.

2.3.3. Alaska

[14] Fire boundary polygons for large fires in Alaska are compiled annually by the Alaskan Fire Service [*Kasischke et al.*, 2002] (available online at http://agdc.usgs.gov/data/blm/fire/index.htm). The daily reports of fire activity from the National Interagency Coordination center (archived online at http://www.cidi.org/wildfire) were used to construct a temporal profile of fire activity for the entire state. The daily reports are part of the operational activity of the Alaska Fire Service, but boundaries of fires are not always updated daily, especially in limited protection areas. In contrast with the other regions in the BWEM-1, temporal profiles were not calculated for individual fires, but instead a single profile for the entire region was applied. This approach likely results in significant errors in the timing of individual fires in Alaska. These errors will be greater at finer spatial and temporal scales, which affects how simulation results for Alaska fire emissions should be interpreted.

2.4. Chemistry and Transport Model

[15] Transport and chemistry of CO emissions were simulated using the University of Maryland CTM [*Allen et al.*, 1996], using assimilated meteorological data from version 3 of the Goddard Earth Observing System Data Assimilation System (GEOS DAS) [*Hou et al.*, 2003]. This model was run with a spatial resolution of 2.5° longitude by 2° latitude, with 35 vertical layers (17 in the troposphere), with CO mixed uniformly through the boundary layer at each model time step. Model output was recorded at 6-hour intervals.

[16] All the principal sources of CO to the atmosphere were included in the CTM simulation, with the exception of CO from soils [*Kuhlbusch et al.*, 1998; *Zepp et al.*, 1997], which are expected to be a minor contributor to overall CO emissions, and for which no comprehensive data source is available. All sources were tagged, permitting accurate calculation of the impacts of each source on total simulated CO. Fossil fuel CO emissions were estimated with the inventory described by *Bey et al.* [2001], with Asian emissions from the inventory of *Streets et al.* [2003] superimposed. CO emissions from biomass burning outside the boreal zone were taken from the Global Fire Emissions Database product, version 1 (http://www.ess.uci.edu/~jranders/readme1.txt). This database uses data from the Tropical Rainfall Monitoring Mission (TRMM) satellite to estimate fire size, location, and timing [*Giglio et al.*, 2003], and estimates fuel consumption using a dynamic vegetation model, the Carnegie-Ames-Stanford Approach (CASA) [*Potter et al.*, 1993]. Details of this dataset can be found in *van der Werf et al.* [2003]. Production of CO from biofuel combustion including agricultural burning and fuelwood use was estimated based on the inventory of *Yevich and Logan* [2003].

[17] In addition to surface sources, the model includes photochemical production of CO from methane oxidation as well as isoprene and terpene oxidation. Methane oxidation was calculated online using fixed methane fields from *Dlugokencky et al.* [1994] and OH fields from *Spivakovsky et al.* [2000]. Production of CO from oxidation of isoprene and terpene was calculated offline using the method of *Allen et al.* [1996].

[18] The principal atmospheric sink of CO is oxidation by hydroxyl, and this sink was calculated online in the CTM. Fixed OH fields from *Spivakovsky et al.* [2000] were used.

2.5. CO Observations

[19] In this study, three different types of CO observations were examined. Properties of each type of measurement are described below.

2.5.1. Surface Flask Measurements

[20] Surface CO measurements from the NOAA Cooperative Air Sampling Network (CASN) were taken from 23 fixed stations north of 30°N during the study period. A quality control process was used to flag measurements unlikely to represent well-mixed air masses [*Novelli and Steele*, 1992]. This process was primarily intended to eliminate influence of local sources, but may remove measurements influenced by large regional pollution plumes. Flagged measurements were not included in this study.

[21] The accuracy and precision of the CASN data are very high. Absolute accuracy was estimated by analytical propagation of errors to be around ±3.5 ppbv for these flask measurements [*Novelli et al.*, 2003]. The precision of the gas chromatography/mercuric oxide reduction method used for CO analysis was determined to be better than 2%

Table 1. Statistics for Daily and Composite Emissions Products[a]

	Percent of HNH Cells With CO Emissions	Mean CO Emissions in Active Grid Cells, g CO $\times 10^9$	95th Percentile of CO Emissions From Active Grid Cells, g CO $\times 10^9$
Daily	0.54%	13.85	70.14
7-day	1.49%	4.98	21.35
30-day	3.21%	2.25	13.70

[a]Statistics were calculated for cells on the 2° latitude by 2.5° longitude daily grid used for input to the chemistry transport model. Statistics shown are for June to August only. HNH is high Northern Hemisphere.

[*Novelli et al.*, 1998]. CTM outputs were matched to flask measurements by sampling model output from the grid cell containing the measurement station at the time step closest to the collection date and time.

2.5.2. Continuous Analyzer Data

[22] High-frequency CO data were obtained from the station at Mace Head, Ireland, part of the AGAGE network [*Prinn et al.*, 2000]. CO concentrations are measured every 40 min using the same analytical method used for the CASN flask measurements [*Derwent et al.*, 2001]. The analyzers are regularly calibrated to standards from CSIRO [*Simmonds et al.*, 1996]. The absolute accuracy of this data is comparable to that of the CASN flask measurements. ''Polluted'' measurements are also flagged in this data set, based on simultaneous measurements of CFCs, which are an indicator of anthropogenic sources. Flagged measurements from this data set were included in the analysis.

[23] CTM outputs were matched to this data by first taking the time series of model output at the grid cell containing the measurement location, and then interpolating to match the observation times. Since CTM output was only generated every six hours, the Mace Head CO measurements have greater temporal detail than the model output.

2.5.3. MOPITT CO Retrievals

[24] Total column (TC) CO retrievals from the MOPITT instrument Level 2, Version 3 data product were used [*Deeter et al.*, 2004; *Deeter et al.*, 2003]. The analysis was limited to retrievals north of 30°N. Retrievals with more than 40% a priori contribution at the 700 hPa nominal level, as well as retrievals with estimated radiometric error greater than 25% (about 10% of HNH retrievals), were excluded. Application of these filters left approximately 36,000 retrievals per day during the study period. Validation exercises comparing MOPITT data to profiles obtained from aircraft sampling give an estimated bias in MOPITT total column CO of $0.7 \times 10^{17} \pm 1.9 \times 10^{17}$ molecules cm^{-2}, which is approximately 5 ± 11% [*Emmons et al.*, 2004].

[25] For comparison with model output, each MOPITT retrieval was matched to its corresponding location on the output grid, and the CTM output from the two nearest output periods was interpolated to yield a simulated vertical profile. This profile was then vertically interpolated to the nominal MOPITT retrieval vertical levels and combined with the MOPITT averaging kernel according to the method described by M. N. Deeter (Calculation and Application of MOPITT Averaging Kernels, 2002, http://www.eos.ucar.edu/mopitt/data/avg_krnls_app.pdf). The result was a simulated MOPITT CO column, from which TC CO was derived using the hydrostatic relation, as described by *Emmons et al.* [2004]. The individual contribution of each simulated CO source to the simulated MOPITT TC CO value was obtained by subtracting the a priori component from each simulated retrieval, using the method of *Arellano et al.* [2004].

3. Results and Discussion

3.1. Temporal Signal in BWEM-1 Daily Data

[26] Daily, 7-day and 30-day average emissions were interpolated to the same $144 \times 91 \times 366$ (2.5° longitude by 2° latitude by 366 days) CTM input grid. Statistics from the comparison of these gridded data sets are presented in Table 1. Temporal smoothing greatly increased the number of cells where fire activity was indicated, resulting in a decrease in the average emissions from each active cell. The 7-day aggregate had less than half the variance of the daily data, and the 30-day aggregate had less than 20% of the initial variance. This result indicates that significant information is lost in aggregation of daily fire data.

[27] To test for evidence of periodicity that might indicate systematically incomplete coverage, time lag autocorrelations were prepared for the daily data. Figure 2 shows lag correlation statistics for Alaska, Canada, and Russia. All of the data showed rapid decay of autocorrelation, which is consistent with scientific understanding of the behavior of large forest fires [*Flannigan and Harrington*, 1988]. The data from Alaska showed some evidence of periodicity, which may indicate a systematic schedule of remapping active fire boundaries. Features at long time lags in the Alaskan data are related to the time elapsed between the few

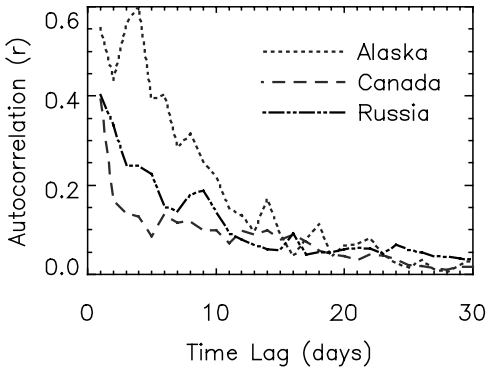

Figure 2. Time lag autocorrelation for gridded daily emissions from Alaska, Canada, and Russia.

Table 2. Contribution of CO From Boreal Forest Fires to Simulated Surface Measurements From CASN and Mace Head[a]

	Daily	7-day	30-day
		CASN (N = 283)	
Mean CO (ppbv)	22.4 ± 15.7	23.3 ± 16.0	22.1 ± 16.7
Difference from daily (ppbv)	-	0.9 ± 4.1	−0.3 ± 9.9
Correlation versus daily (r)	-	0.97	0.81
		Mace Head (N = 2700)	
Mean CO (ppbv)	23.0 ± 9.7	23.8 ± 10.1	20.6 ± 8.1
Difference from daily (ppbv)	-	0.7 ± 1.5	−2.4 ± 6.2
Correlation versus daily (r)	-	0.99	0.78

[a]Confidence limits are ±1σ. All correlations are significant to $p < 0.001$; CASN is the NOAA Cooperative Air Sampling Network.

major fires of the 2000 season. The Russian data showed qualitative evidence of periodicity, but the autocorrelation did not exceed 0.2 after five days. The lag correlation patterns observed in this data did not suggest sampling issues of the type encountered in the WFW data for the tropics [*Heald et al.*, 2003]. This test does not demonstrate that the BWEM-1 data had complete daily sampling, only that the data did not show systematic reduction of sampling rate. The rate of decay observed in Figure 2 reflects both incomplete sampling due to cloud contamination and the actual persistence of fire activity.

3.2. Signal of Daily Variability in Atmospheric Measurements

[28] The atmospheric measurements used in this study had very different sampling properties, and were not expected to have the same response to the high-frequency signal in the emissions source. Each type of atmospheric measurement is considered separately in this section.

3.2.1. CASN Flask Measurements

[29] Table 2 presents statistical measures of the simulated boreal contribution to surface CO measurements for the daily and aggregated simulations, as well as the mean difference between daily and aggregate simulations and the correlation between daily and aggregate simulations. Out of 283 simulated CASN observations, the daily and 7-day simulations differed by more than 10% on only 2 occasions. The correlations among simulations were extremely strong, showing that the daily and 7-day simulations were nearly identical in this sample, and the 30-day simulation differed only slightly.

3.2.2. Mace Head Observations

[30] Table 2 presents the results of a statistical analysis of the simulated contribution of boreal forest fires to CO observations from Mace Head from the daily, 7-day and 30-day simulations. While the boreal CO contributed about 25% of the total simulated CO during the study period, the distance between the source and the measurement location reduced the influence of high-frequency variability in the source. The maximum deviation between daily and 7-day simulations during the study period was only 5% of the observed CO value.

3.2.3. MOPITT Retrievals

[31] MOPITT data have a spatial coverage and data volume far greater than the other two measurement types, but with lesser accuracy and precision. The daily and 7-day simulations had very small differences in nearly all of the data, but the data volume from MOPITT was sufficient to find a large sample of retrievals where the differences were large enough to analyze. For this study, we analyzed the complete set of retrievals after applying the filters described in section 2.5.3, and also a subset of retrievals with the highest contrast between simulations. This subset was selected by calculating the difference between daily and 7-day simulations for each simulated retrieval, and dividing this value by the estimated error from the MOPITT data. When a threshold of twice the estimated error was applied, fewer than 1% of the retrievals remained. The distribution of these retrievals is determined both by the strength of the simulated boreal forest fire CO source and the error of the retrieval. Figure 3 shows the spatial distribution of the 35,323 retrievals in the high-contrast subset. Most of these measurements were concentrated near the source (compare to Figure 1).

[32] Table 3 lists the magnitude of the boreal fire CO signal and the differences between simulations for different geographic regions as well as for the high-contrast subset. The fraction of simulated nonboreal CO is an approximate

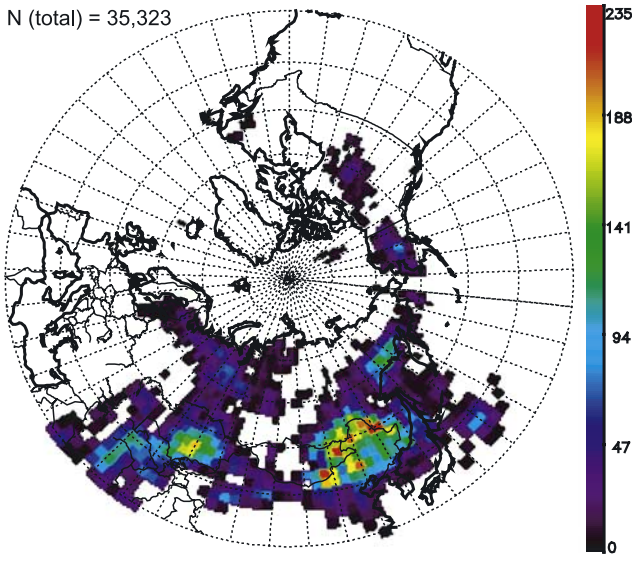

Figure 3. Spatial distribution of CO retrievals in the "daily versus 7-day" high-contrast subset, where the daily and 7-day simulations differed by more than twice the estimated error in the Measurement of Pollution in the Troposphere (MOPITT) retrieval.

Table 3. Results of Model Simulation of Boreal Forest Fire CO Influence on MOPITT Total Column CO Retrievals[a]

	N	Mean of Daily Simulated, molecules $cm^{-2} \times 10^{-17}$	Percent of Total Simulated Nonboreal CO		
			Daily	7-day	30-day
HNH	3251253	2.33 ± 2.59	15.6 ± 17.2	15.7 ± 14.7	15.7 ± 13.9
Russia	269944	3.84 ± 2.43	26.1 ± 15	26.8 ± 17.6	28.6 ± 15.1
Canada	296097	3.27 ± 1.35	22.8 ± 9.1	23.1 ± 9.3	23.6 ± 9.5
Alaska	284318	3.76 ± 5.04	25.3 ± 33.5	25.4 ± 23.4	25.2 ± 23.6
High-contrast	35323	12.6 ± 15.5	84.1 ± 103.6	74.6 ± 64.9	56 ± 52.1

[a]Confidence limits are $\pm 1\sigma$. MOPITT is Measurement of Pollution in the Troposphere. HNH is high Northern Hemisphere.

figure, because the convolution of the a priori profile in the MOPITT retrieval prevents exact determination of individual source contributions.

3.3. Effect of Source Resolution on Agreement Between Model and Measurements

[33] The CTM simulation of boreal forest fire CO was compared with observations by first comparing the observations with the CTM simulation with all sources excluding boreal forest fires, followed by comparison of the simulated boreal CO compared with the residuals remaining after subtraction of the simulated CO from other sources.

[34] The agreement between simulated CO from boreal forest fires and observations was thus dependent on the accuracy of the simulation of nonboreal sources, but this was unavoidable. The accuracy of the simulated nonboreal sources was sufficient to justify quantitative evaluation of the relative results obtained with different simulations of the boreal source. Note that for the estimates of absolute bias obtained from this comparison, biases in boreal and nonboreal sources could not be disentangled. Therefore, the comparison of simulated boreal forest fire CO to residuals from observations centered on two statistical measures, the scatter in model errors (represented by the standard deviation of errors), and the overall correlation between model and observations (represented by the r value).

3.3.1. Surface CO Observations From Flask Data

[35] Table 4 presents the statistical comparison between the simulated and observed surface CO observations from the CASN flask network. The daily and composite simulations were nearly identical. Differences among simulations in the agreement with observations were very minor. This result demonstrates the effectiveness of the filtering algorithm used to remove plume-influenced data from the CASN data set. Boreal forest fire CO made up a significant fraction of the CO in these measurements, but the lack of sensitivity to high-frequency variability in this source indicates that the measurements effectively sampled only well-mixed air masses.

3.3.2. CO Observations From Mace Head

[36] Figure 4 shows the time series of CO observations from Mace Head. The variability in CO observed at Mace Head during the study period was almost entirely due to intrusion of polluted air masses onto the clean marine background. During much of the month of June, the model showed substantial CO from boreal forest fires, and the features of this CO enhancement were reflected in the observations. After June, the CO contribution from boreal forest fires was generally small. As expected the daily and 7-day simulations were nearly identical. Some differences in larger features can be discerned between the 30-day and higher-resolution simulations.

[37] Table 4 also presents results from statistical comparison of CTM simulations and Mace Head observations. Both daily and 7-day simulations produced better correlations with observations, and smaller scatter of model errors, compared with the simulation using 30-day aggregate data. This is noteworthy because the higher-resolution simulations had greater variance to begin with.

3.3.3. MOPITT CO Retrievals

[38] Table 5 presents error statistics for the model simulation of CO from nonboreal sources. Without the CO source from boreal fires, the model underestimated MOPITT CO throughout the HNH. The high-contrast subset showed higher bias and more scatter in model errors, consistent with a larger and less well-mixed contribution from boreal forest fires.

Table 4. Comparison of CTM Simulation to CASN and Mace Head Surface Observations of CO[a]

	Mean Bias, ppbv[b]	SD of Bias	Correlation[c]
	CASN Data (N = 283)		
Nonboreal Sources	6.45	39.0	0.56
Daily simulated boreal forest fire source[d]	−15.9	38.9	0.21
7-day simulated boreal forest fire source[d]	−16.8	38.6	0.23
30-day simulated boreal forest fire source[d]	−15.6	38.6	0.23
	Mace Head Data (N = 2700)		
Nonboreal sources	−2.0	15.8	0.77
Daily simulated boreal forest fire source[d]	−25.0	15.9	0.30
7-day simulated boreal forest fire source[d]	−25.7	15.9	0.31
30-day simulated boreal forest fire source[d]	−22.6	16.7	0.14

[a]CTM is chemistry and transport model. CASN is NOAA Cooperative Air Sampling Network.
[b]Negative values indicate overestimation by the model.
[c]All CASN correlations are significant to $p < 0.01$ or better. Estimating significance of Mace Head correlations is more difficult due to temporal autocorrelation of 40-min data.
[d]Comparison between observations and boreal source simulations was done using the residuals after subtraction of simulated nonboreal CO.

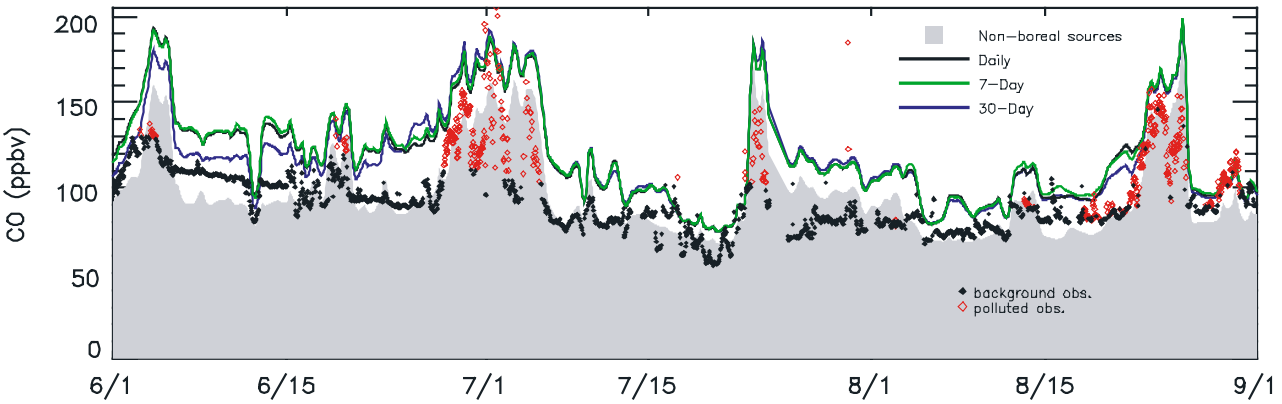

Figure 4. Time series of CO observations (points) and simulated CO (lines) from Mace Head, Ireland.

[39] Table 5 also presents the results of the comparison between the residuals obtained by subtraction of the simulated CO from nonboreal sources from the MOPITT data and the simulated boreal forest fire CO. Temporal resolution had no effect on agreement over the entire HNH. The simulated boreal source agreed poorly with MOPITT residuals over North America, and effects of temporal resolution cannot be discerned there. Over Russia, and in the high-contrast subset, the higher-resolution sources correlated better with observations than the 30-day aggregate source. The higher variability of the high-resolution simulations was somewhat reflected in observations over Russia, but the high-contrast subset of the simulation contained substantial variability that was not reflected in the observations. The error statistics for the high-contrast measurements indicated that aggregation to monthly averages removed useful information from atmospheric simulations. This comparison permits no conclusions about the quality of daily data, as comparable results are obtained with 7-day averages.

4. Summary and Conclusions

[40] A daily database of CO emissions from boreal forest fires was used as input to a chemistry and transport model, to evaluate the impact of daily emissions data on simulations of CO transport and evolution. Aggregation of daily data to 7-day averages reduced the variance in the data by more than half. Some evidence of periodicity was found in the Alaskan emissions data, but otherwise autocorrelations were small and decayed rapidly, indicating that any incompleteness in sampling of fire activity was not systematic. This method did not determine the sampling efficiency of the data sources used, but ruled out systematic detection problems such as those described by *Heald et al.* [2003].

[41] Filtering performed on the CASN flask data is intended to remove the influence of local sources, but also has the effect of eliminating any high-frequency signal. The boreal fire CO source was a significant contributor to these measurements, but the daily and aggregate simulations produced indistinguishable results. This demonstrates the effectiveness of the filtering method at producing a data set sampling only well-mixed air masses, and suggests limits to the applicability of these data for validation of high-resolution transport simulations.

[42] The in situ measurements from Mace Head are largely free of local influence, but the variability in CO during that period was largely related to intrusions of polluted continental air masses. The 30-day simulation

Table 5. Statistical Comparison of CTM Simulation to MOPITT Total Column CO Retrievals

	Entire HNH	Russia	Canada	Alaska	High-Contrast
			Nonboreal CO		
Mean bias (10^{17} molecules cm^{-2})	5.2	5.7	5.7	6.1	6.7
SD of error $\times$ 10^{-17}	2.5	2.3	2.2	2.2	3.5
R	0.59	0.60	0.65	0.61	0.60
			Daily[a]		
Mean bias (10^{17} molecules cm^{-2})	2.4	1.9	2.4	2.3	−3.5
SD of error $\times$ 10^{-17}	2.7	3.6	2.4	2.8	9.7
R	0.34	0.29	0.14	0.17	0.50
			7-day[a]		
Mean bias (10^{17} molecules cm^{-2})	2.3	1.9	2.3	2.2	−3.4
SD of error $\times$ 10^{-17}	2.7	3.0	2.5	3.0	7.2
R	0.35	0.30	0.13	0.16	0.46
			30-day[a]		
Mean bias (10^{17} molecules cm^{-2})	2.4	1.9	2.3	2.0	−1.2
SD of error $\times$ 10^{-17}	2.7	3.5	2.4	2.8	6.5
R	0.32	0.19	0.18	0.16	0.31

[a]Simulated boreal forest fire CO was compared to residuals of MOPITT total column CO retrievals after subtraction of simulated nonboreal sources.

showed significant differences from the higher-resolution simulations in these data, and the agreement between the model and observations was worse for the 30-day aggregate source than for the higher-resolution sources.

[43] The simulated MOPITT data showed that the signal from high-frequency variability in the emissions source dwindled rapidly with increasing distance from the emissions source. The daily and 7-day simulations differed by more than twice the estimated error of the MOPITT retrievals in a small subset of the data, roughly 1% of the 3.2 million retrievals over the high Northern Hemisphere during the study period. As with the Mace Head data, the 30-day simulation had generally worse agreement with observations, except over North America, where all simulations of the boreal source produced poor agreement with observations.

[44] The importance of resolving the temporal profile of fire events for transport investigations is intuitively obvious, but the results of this study indicate that atmospheric measurements are not necessarily sensitive to high-frequency variability in surface sources. Where measurements have sensitivity, however, our results indicate that significant information is lost when using monthly average sources for atmospheric simulations. The simulations in this study did not produce better results with daily data compared with 7-day averages. This might indicate the limits of the input observations of fire activity, as well as the limitations of transport accuracy for this type of simulation. Further research is needed to determine whether current data sources can produce a daily product that gives significantly better results than weekly averages.

[45] **Acknowledgments.** This research was supported by a NASA Earth System Science Fellowship and the NASA Interdisciplinary Science Program, as well as the Office of Naval Research code 32.

References

Allen, D. J., P. Kasibhatla, A. M. Thompson, R. B. Rood, B. G. Doddridge, K. E. Pickering, R. D. Hudson, and S. J. Lin (1996), Transport-induced interannual variability of carbon monoxide determined using a chemistry and transport model, *J. Geophys. Res.*, *101*, 28,655–28,669.

Arellano, A. F., Jr., P. S. Kasibhatla, L. Giglio, G. R. van der Werf, and J. T. Randerson (2004), Top-down estimates of global CO sources using MOPITT measurements, *Geophys. Res. Lett.*, *31*, L01104, doi:10.1029/2003GL018609.

Bey, I., D. J. Jacob, R. M. Yantosca, J. A. Logan, B. D. Field, A. M. Fiore, Q. B. Li, H. G. Y. Liu, L. J. Mickley, and M. G. Schultz (2001), Global modeling of tropospheric chemistry with assimilated meteorology: Model description and evaluation, *J. Geophys. Res.*, *106*, 23,073–23,095.

Damoah, R., N. Spichtinger, R. Servranckx, M. Fromm, E. W. Eloranta, I. A. Razenkov, P. James, M. Shulski, C. Forster, and A. Stohl (2006), A case study of pyro-convection using transport model and remote sensing data, *Atmos. Chem. Phys.*, *6*, 173–185.

Deeter, M. N., et al. (2003), Operational carbon monoxide retrieval algorithm and selected results for the MOPITT instrument, *J. Geophys. Res.*, *108*(D14), 4399, doi:10.1029/2002JD003186.

Deeter, M. N., L. K. Emmons, D. P. Edwards, J. C. Gille, and J. R. Drummond (2004), Vertical resolution and information content of CO profiles retrieved by MOPITT, *Geophys. Res. Lett.*, *31*, L15112, doi:10.1029/2004GL020235.

Derwent, R. G., W. J. Collins, C. E. Johnson, and D. S. Stevenson (2001), Transient behaviour of tropospheric ozone precursors in a global 3-D CTM and their indirect greenhouse effects, *Clim. Change*, *49*(4), 463–487.

Dlugokencky, E. J., L. P. Steele, P. M. Lang, and K. A. Masarie (1994), The growth rate and distribution of atmospheric methane, *J. Geophys. Res.*, *99*, 17,021–17,044.

Duncan, B. N., R. V. Martin, A. C. Staudt, R. Yevich, and J. A. Logan (2003), Interannual and seasonal variability of biomass burning emissions constrained by satellite observations, *J. Geophys. Res.*, *108*(D2), 4100, doi:10.1029/2002JD002378.

Emmons, L. K., et al. (2004), Validation of Measurements of Pollution in the Troposphere (MOPITT) CO retrievals with aircraft in situ profiles, *J. Geophys. Res.*, *109*, D03309, doi:10.1029/2003JD004101.

Eva, H., and E. F. Lambin (1998), Remote sensing of biomass burning in tropical regions: Sampling issues and multisensor approach, *Remote Sens. Environ.*, *64*, 292–315.

Flannigan, M. D., and J. B. Harrington (1988), A study of the relation of meteorological variables to monthly provincial area burned by wildfire in Canada (1953–1980), *J. Appl. Meteorol.*, *27*, 441–452.

Fraser, R. H., Z. Li, and J. Cihlar (2000), Hotspot and NDVI differencing synergy (HANDS): A new technique for burned area mapping over boreal forest, *Remote Sens. Environ.*, *74*, 362–376.

Fromm, M., R. Bevilacqua, R. Servranckx, J. Rosen, J. P. Thayer, J. Herman, and D. Larko (2005), Pyro-cumulonimbus injection of smoke to the stratosphere: Observations and impact of a super blowup in northwestern Canada on 3–4 August 1998, *J. Geophys. Res.*, *110*, D08205, doi:10.1029/2004JD005350.

Giglio, L., J. D. Kendall, and R. Mack (2003), A multi-year active fire dataset for the tropics derived from the TRMM VIRS, *Int. J. Remote Sens.*, *24*(22), 4505–4525.

Heald, C. L., D. J. Jacob, P. I. Palmer, M. J. Evans, G. W. Sachse, H. B. Singh, and D. R. Blake (2003), Biomass burning emission inventory with daily resolution: Application to aircraft observations of Asian outflow, *J. Geophys. Res.*, *108*(D21), 8811, doi:10.1029/2002JD003082.

Hou, A. Y., S. Q. Zhang, and O. Reale (2003), Variational continuous assimilation on TMI and SSM/I rain rates: Impact on GEOS-3 hurricane analyses and forecasts, *Mon. Weather Rev.*, *132*, 2094–2109.

Kasischke, E. S., D. Williams, and D. Barry (2002), Analysis of the patterns of large fires in the boreal forest region of Alaska, *Int. J. Wildland Fire*, *11*(2), 131–144.

Kasischke, E. S., J. H. Hewson, B. Stocks, G. van der Werf, and J. Randerson (2003), The use of ATSR active fire counts for estimating relative patterns of biomass burning: A study from the boreal forest region, *Geophys. Res. Lett.*, *30*(18), 1969, doi:10.1029/2003GL017859.

Kasischke, E. S., E. J. Hyer, P. C. Novelli, L. P. Bruhwiler, N. H. F. French, A. I. Sukhinin, J. H. Hewson, and B. J. Stocks (2005), Influences of boreal fire emissions on Northern Hemisphere atmospheric carbon and carbon monoxide, *Global Biogeochem. Cycles*, *19*, GB1012, doi:10.1029/2004GB002300.

Kaufman, Y. J., D. D. Herring, K. J. Ranson, and G. J. Collatz (1998), Earth Observing System AM1 mission to Earth, *IEEE Trans. Geosci. Remote Sens.*, *36*(4), 1045–1055.

Kuhlbusch, T. A. J., R. G. Zepp, W. L. Miller, and R. A. Burke (1998), Carbon monoxide fluxes of different soil layers in upland Canadian boreal forests, *Tellus, Ser. B*, *50*(4), 353–365.

Li, Z. Q., J. Cihlar, L. Moreau, F. T. Huang, and B. Lee (1997), Monitoring fire activities in the boreal ecosystem, *J. Geophys. Res.*, *102*, 29,611–29,624.

Malingreau, J. P., and J.-M. Grégoire (1996), Developing a global vegetation fire monitoring system for global change studies: A framework, in *Biomass Burning and Global Change*, edited by J. S. Levine, pp. 14–24, MIT Press, Cambridge, Mass.

Novelli, P. C., and L. P. Steele (1992), Mixing ratios of carbon monoxide in the troposphere, *J. Geophys. Res.*, *97*, 20,731–20,750.

Novelli, P. C., K. A. Masarie, and P. M. Lang (1998), Distributions and recent changes of carbon monoxide in the lower troposphere, *J. Geophys. Res.*, *103*, 19,015–19,033.

Novelli, P. C., K. A. Masarie, P. M. Lang, B. D. Hall, R. C. Myers, and J. W. Elkins (2003), Reanalysis of tropospheric CO trends: Effects of the 1997–1998 wildfires, *J. Geophys. Res.*, *108*(D15), 4464, doi:10.1029/2002JD003031.

Potter, C. S., J. T. Randerson, C. B. Field, P. A. Matson, P. M. Vitousek, H. A. Mooney, and S. A. Klooster (1993), Terrestrial ecosystem production: A process model based on global satellite and surface data, *Global Biogeochem. Cycles*, *7*, 811–842.

Prinn, R. G., et al. (2000), A history of chemically and radiatively important gases in air deduced from ALE/GAGE/AGAGE, *J. Geophys. Res.*, *105*, 17,751–17,792.

Prins, E. M., and W. P. Menzel (1994), Trends in South American biomass burning detected with the GOES visible infrared spin scan radiometer atmospheric sounder from 1983 to 1991, *J. Geophys. Res.*, *99*, 16,719–16,735.

Reid, J. S., E. M. Prins, D. L. Westphal, C. C. Schmidt, K. A. Richardson, S. A. Christopher, T. F. Eck, E. A. Reid, C. A. Curtis, and J. P. Hoffman (2004), Real-time monitoring of South American smoke particle emissions and transport using a coupled remote sensing/box-model approach, *Geophys. Res. Lett.*, *31*, L06107, doi:10.1029/2003GL018845.

Simmonds, P. G., R. G. Derwent, A. McCulloch, S. O'Doherty, and A. Gaudry (1996), Long-term trends in concentrations of halocarbons and radiatively active trace gases in Atlantic and European air masses monitored at Mace Head, Ireland from 1987–1994, *Atmos. Environ.*, *30*(23), 4041–4063.

Spivakovsky, C. M., et al. (2000), Three-dimensional climatological distribution of tropospheric OH: Update and evaluation, *J. Geophys. Res.*, *105*, 8931–8980.

Stocks, B. J., B. D. Amiro, and B. D. Wotton (2002), Large forest fires in Canada 1959–1997, *J. Geophys. Res.*, *108*(D1), 8149, doi:10.1029/2001JD000484.

Streets, D. G., et al. (2003), An inventory of gaseous and primary aerosol emissions in Asia in the year 2000, *J. Geophys. Res.*, *108*(D21), 8809, doi:10.1029/2002JD003093.

Stroppiana, D., S. Pinnock, and J. M. Gregoire (2000), The global fire product: Daily fire occurrence from April 1992 to December 1993 derived from NOAA AVHRR data, *Int. J. Remote Sens.*, *21*(6–7), 1279–1288.

Sukhinin, A. I., et al. (2004), AVHRR-based mapping of fires in Russia: New products for fire management and carbon cycle studies, *Remote Sens. Environ.*, *93*, 546–564.

van der Werf, G. R., J. T. Randerson, G. J. Collatz, and L. Giglio (2003), Carbon emissions from fires in tropical and subtropical ecosystems, *Global Change Biol.*, *9*(4), 547.

Yevich, R., and J. A. Logan (2003), An assessment of biofuel use and burning of agricultural waste in the developing world, *Global Biogeochem. Cycles*, *17*(4), 1095, doi:10.1029/2002GB001952.

Yurganov, L. N., et al. (2004), A quantitative assessment of the 1998 carbon monoxide emission anomaly in the the Northern Hemisphere based on total column and surface concentration measurements, *J. Geophys. Res.*, *109*, D15305, doi:10.1029/2004JD004559.

Zepp, R. G., W. L. Miller, M. A. Tarr, R. A. Burke, and B. J. Stocks (1997), Soil-atmosphere fluxes of carbon monoxide during early stages of post-fire succession in upland Canadian boreal forests, *J. Geophys. Res.*, *102*, 29,301–29,311.

D. J. Allen, Department of Atmospheric and Oceanic Science, University of Maryland, College Park, MD 20742, USA.

E. J. Hyer, Marine Meteorology Division, Naval Research Laboratory, 7 Grace Hopper Avenue, Stop 2, Monterey, CA 93943, USA. (edward.hyer@nrlmry.navy.mil)

E. S. Kasischke, Department of Geography, University of Maryland, College Park, MD 20742, USA.